

## The Crystal Structure of Baddeleyite (Monoclinic $ZrO_2$ ) and its Relation to the Polymorphism of $ZrO_2$ \*

BY DEANE K. SMITH AND HERBERT W. NEWKIRK

Lawrence Radiation Laboratory, University of California, Livermore, California, U.S.A.

(Received 15 June 1964 and in revised form 5 October 1964)

The crystal structure of baddeleyite has been redetermined using new X-ray data collected from a synthetic single crystal. A three-dimensional least-squares refinement reconfirms the structure determined by McCullough & Trueblood (*Acta Cryst.* **12**, 507 (1959)).

The  $P2_1/c$  unit cell contains 4  $ZrO_2$ . All the atoms are in the general positions with the Zr at  $x=0.2758$ ,  $y=0.0411$ , and  $z=0.2082$ ;  $O_I$  at  $x=0.070$ ,  $y=0.342$ ,  $z=0.341$ ; and  $O_{II}$  at  $x=0.442$ ,  $y=0.755$ ,  $z=0.179$ . The Zr is in sevenfold coordination, with Zr–O distances ranging from 2.05 Å to 2.28 Å. The  $O_I$  is coordinated to three Zr atoms in an approximately planar configuration. The  $O_{II}$  is four-coordinated in a distorted tetrahedral configuration.

The structure can be described as a distortion of the cubic fluorite ( $CaF_2$ ) structure. The  $O_{II}$  atoms lie in a plane parallel to (100) and form a slightly distorted square array. The Zr atoms lying above and below the  $O_{II}$  planes are positioned alternately above or below a square of  $O_{II}$  atoms. The  $O_I$  atoms also lie in a plane parallel to (100) but are arranged irregularly so that only three are coordinated to any one Zr atom.

The common polysynthetic (100) twinning is discussed in terms of the layer arrangement of atoms and a probable arrangement at the composition plane is proposed. The most likely structural rearrangements in the polymorphic inversion series monoclinic–tetragonal–cubic is also discussed in terms of the layering parallel to (100).

### Introduction

The crystal structure of baddeleyite has been of interest since the early work of Yardley (Lonsdale) (1926). Her work determined the  $P2_1/c$  space group and the presence of 4  $ZrO_2$  in the unit cell. The suggestion was made that the structure was probably some distortion of the fluorite structure. Using Yardley's data, Naray-Szabo (1936) proposed a structure; this proposed structure, however, had unsatisfactory packing and unreasonable bond distances. McCullough & Trueblood (1959) collected new data from some natural crystal fragments which appeared free of the twinning that is present in most if not all natural crystals. Although the McCullough & Trueblood structure is very reasonable, it was based on projection data only. A refinement of the structure using complete three-dimensional data was, therefore, indicated.

The importance of knowing details of the monoclinic  $ZrO_2$  structure is shown by the increasing interest in understanding the monoclinic–tetragonal–cubic phase transition series and its relations to the stabilization of the cubic phase in  $ZrO_2$  ceramics. The monoclinic–tetragonal inversion has been the subject of several recent investigations by Baun (1963), Garrett (1964) and others. The tetragonal–cubic transformation has been studied by Cohen & Schaner (1963) and Smith and Cline (1962); however, the existence of the

cubic phase as a stable phase for pure stoichiometric  $ZrO_2$  has been questioned, particularly by Weber (1962). The crystal structure of the tetragonal modification has been reported by Teufer (1962).

### Crystal growth

Single crystals of monoclinic  $ZrO_2$  up to 1 mm in maximum dimension were obtained from mixtures of  $ZrO_2$  and  $Li_2Mo_2O_7$  flux prepared from reagent-grade chemicals. The mixtures were placed in 100-ml platinum crucibles which were covered with tightly fitted lids to minimize losses of  $MoO_3$  by evaporation. The amount of dry mixture used was sufficient to fill the entire volume of the crucible when packed tightly. A satisfactory prescription proved to be 10 g  $ZrO_2$  (20.5 mole%) in 100 g  $Li_2Mo_2O_7$ . The filled crucibles were placed on  $Al_2O_3$  setter batts, inserted in a muffle furnace, and heated to 1400 °C. After soaking for 4 hours, a gradient of 10 °C was imposed on the crucible by lowering the power on the silicon carbide heating elements at the bottom of the muffle furnace. The crucible was then cooled at the rate of 4 °C per hour. The crucibles were usually withdrawn when the temperature reached 900 °C. The flux was poured off, and the crystals were harvested by leaching the remaining contents of the crucible with hot water\*.

\* Work performed under the auspices of the U.S. Atomic Energy Commission.

\* Some crystals grown by decomposition of  $ZrF_4$  were obtained from Mr Cabel Finch of the Oak Ridge National Laboratory. Unfortunately, all of these crystals were twinned.

### Locating untwinned crystals

Twinning in monoclinic ZrO<sub>2</sub> on (100) is so common that crystals free of twinning are very rare. The crystals obtained from the growth in lithium molybdate fluxes were all about the same size and possessed the same general habit. Crystals with the forms {100}, {110} and {011} about equally developed invariably showed the characteristic polysynthetic twinning on (100). This twinning was usually obvious in polarized light, but some crystals of the same habit had to be examined with the Buerger precession camera before the twinning was observed.

Two single crystals free of twinning were obtained by examining crystals where the {001} and {110} forms were more fully developed than the other forms. This growth produced crystals with a more cubic habit which, when examined with the Buerger precession camera, proved free of detectable twinning. One of these two crystals was used for the structure analysis.

### X-ray data

The single crystal was first examined with the Buerger precession camera using Mo K $\alpha$  radiation. The (*h*0 $l$ ) zone showed no evidence of twinning even with exposures as long as 50 hours. The crystal was then transferred to a single-crystal orienter mounted on a G.E. XRD5 spectrogoniometer. The cell constants reported by Adam & Rogers (1959) and given in Table 1 were used to calculate the goniostat settings. These calculated coordinates proved adequate to locate the intensity maxima; consequently, no further refinement of the unit-cell dimensions was made.

Table 1. *Crystallographic data for monoclinic ZrO<sub>2</sub>*

Space group	McCullough & Trueblood (1959)	Adam & Rogers (1959)
	Natural ZrO <sub>2</sub> (+2 mol. %HfO <sub>2</sub> ) <i>P</i> 2 <sub>1</sub> / <i>c</i>	Synthetic ZrO <sub>2</sub> <i>P</i> 2 <sub>1</sub> / <i>c</i>
<i>a</i>	5·169 ± 8 Å	5·145 ± 5 Å
<i>b</i>	5·232 ± 8	5·2075 ± 5
<i>c</i>	5·341 ± 8	5·3107 ± 5
$\beta$	99° 15' ± 10'	99° 14' ± 5'
<i>V</i> (Å <sup>3</sup> )	142·36 Å <sup>3</sup>	140·24 Å <sup>3</sup>
$\rho$ (calc)	5·826 g.cm <sup>-3</sup>	5·836 g.cm <sup>-3</sup>

With Mo K $\alpha$  radiation, a total of 1473 independent reflections within the sphere ( $\sin \theta$ )/ $\lambda = 1\cdot1 \text{ \AA}^{-1}$  were measured by counting at the peak positions for time intervals of 10 to 40 seconds depending on the counting rate. The background was measured at several  $\chi$  and  $\varphi$  settings as a function of  $2\theta$ . The  $\varphi$  dependence appeared negligible. A general background curve in terms of  $\chi$  and  $2\theta$  was established and applied to each reflection. The  $\alpha_1\alpha_2$  resolution was corrected with the curve established by Tulinsky, Worthington & Pignataro (1959). The data were also corrected for the Lorentz-polarization effect.

No correction for absorption was applied to the data. The linear absorption coefficient is 7·1 mm<sup>-1</sup>; thus the optimum size,  $\frac{1}{2}\mu$ , is 0·07 mm. The size of the crystal used in this study was 0·10 × 0·10 × 0·12 mm. During the alignment of the crystal on the goniostat a 10% variation in intensity as a function of  $2\theta$  for the 100 reflection was observed. This variation is indicative of a significant absorption effect, and undoubtedly a better fit between observed and calculated structure factors would be obtained by the use of a correction.

### Refinement of the structure

The positional parameters reported by McCullough & Trueblood were used as the starting point for the refinement of the crystal structure. Using the least-squares refinement program of Gantzel, Sparks & Trueblood (1961), four cycles were sufficient to produce no significant changes in the parameters. The scattering factor curves derived by Thomas & Umeda (1957) were used for Zr. Curves for both neutral Zr and Zr<sup>4+</sup> were used both with and without the dispersion correction of Dauben & Templeton (1955). (Because the artificial crystals were prepared from nuclear-grade hafnium-free zirconia, no modification of the Zr scattering factor curves for Hf content was required.) The scattering curve for neutral oxygen was taken from Hoerni & Ibers (1954). The O<sup>2-</sup> curve was obtained by modifying the Hoerni & Ibers curve for neutral oxygen by the difference between the oxygen and oxide ion scattering factors of James & Brindley (1931).

The best fit of observed and calculated structure factors was obtained with the Zr<sup>4+</sup> scattering-factor curve without dispersion corrections. The values of the index

Table 2. *Refined atomic coordinates for monoclinic ZrO<sub>2</sub>\**

	Zr	O <sub>I</sub>	O <sub>II</sub>
<i>x</i>	(0·2758) 0·2758 ± 2	(0·069) 0·0703 ± 15	(0·451) 0·4423 ± 15
<i>y</i>	(0·0404) 0·0411 ± 2	(0·342) 0·3359 ± 14	(0·758) 0·7549 ± 14
<i>z</i>	(0·2089) 0·2082 ± 2	(0·345) 0·3406 ± 13	(0·479) 0·4789 ± 13
<i>B</i>	0·303	0·317	0·229
<i>B</i> <sub>11</sub>	0·0029	0·0098	0·0102
<i>B</i> <sub>22</sub>	-0·0008	0·0024	0·0025
<i>B</i> <sub>33</sub>	0·0013	0·0038	0·0017
<i>B</i> <sub>12</sub>	-0·0003	0·0028	0·0013
<i>B</i> <sub>13</sub>	0·0016	-0·0019	0·0020
<i>B</i> <sub>23</sub>	0·0003	-0·0045	0·0007

\* The coordinates in parentheses are the values reported by McCullough & Trueblood (1959).

Table 3. The observed and calculated structure factors for monoclinic ZrO2

Table with multiple columns listing structure factors for various h, k, l values. Includes sub-titles like H,K=0,0, H,K=0,1, etc., and numerical values for each reflection. The table is organized into columns and rows based on h, k, l values, with some columns starting with a '10' or '11' indicating the h value.



$R = 100 \Sigma ||F_o| - |F_c|| / \Sigma |F_o|$  were 9.2, 8.6, 9.4, and 9.3 respectively, using the  $Zr^0$  and  $Zr^{4+}$  curves without and with dispersion corrections. The use of the various scattering-factor curves resulted in no significant parameter differences even though the temperature factors showed the expected large deviations. The final parameters are given in Table 2. No explanation can be given as to why the best fit should be obtained without dispersion corrections.

The first sequence of refinements used only isotropic temperature factors. Attempts to refine using anisotropic temperature factors again resulted in lower  $R$  values where no dispersion correction was used, but some of the  $B_{ii}$  terms became zero or very slightly negative. One set of results for  $Zr^{4+}$  including dispersion have been included in Table 2. A negative  $B_{ii}$  term has no physical significance, and its interpretation

has not yet been understood. The correlation matrix does not indicate strong parameter interaction with any other parameter. Possibly the errors introduced by the lack of an absorption correction are to be suspected. Extinction effects could also be reflected in the anomalous temperature parameters, but it is doubtful if such effects are that significant. Only the very strongest reflections appeared to be affected by extinction, and the total number is less than one per cent of the observed data. Other possibilities such as multiple reflections would only affect a small percentage of the observed intensities and are considered insignificant.

A complete list of the observed and calculated structure factors is given in Table 3.

Figs. 1 and 2, reproduced from McCullough & Trueblood, show the final structure of monoclinic  $ZrO_2$ . The coordinates obtained in the present study are only slightly altered from those obtained in their previous study, and the general aspects of structure as described by them are still valid. The complete list of important distances is given in Table 4.

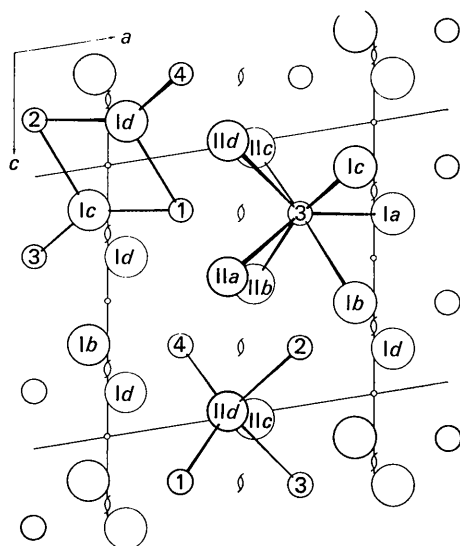


Fig. 1. Projection of the crystal structure of baddeleyite along the  $b$  axis. (From McCullough & Trueblood).

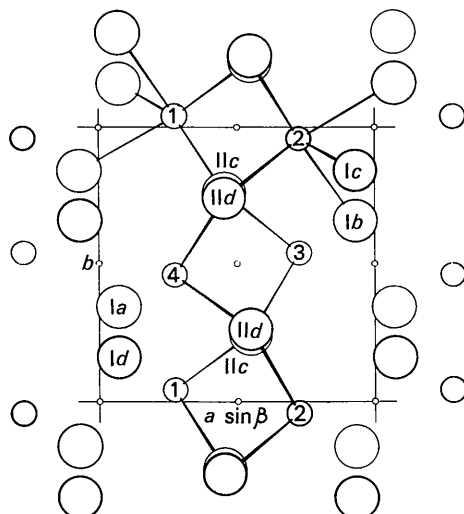


Fig. 2. Projection of the crystal structure of baddeleyite along the  $c$  axis. (From McCullough & Trueblood).

Table 4. Interatomic distances ( $\text{\AA}$ ) in monoclinic  $ZrO_2$

$$\sigma(Zr-O) = 0.007 \text{ \AA} \quad \sigma(O-O) = 0.014 \text{ \AA}$$

(a) Zr-O distances in the Zr(3) coordination polyhedron

Zr	O	Distance	Zr	O	Distance
3	Ia	2.057	3	IIa	2.189
3	Ib	2.163	3	IIb	2.220
3	Ic	2.051	3	IIc	2.151
			3	II d	2.285

(b) O-O distances in the Zr(3) coordination polyhedron

O	O	Distance	O	O	Distance
Ia	Ib	2.589	Ib	IIb	2.918
Ia	Ic	2.829	Ic	IIa	2.581
Ib	Ic	2.802	IIa	IIb	2.722
Ia	IIb	2.985	IIa	IIb	2.658
Ia	IIc	2.929	IIb	IIc	2.658
Ib	IIa	2.581	IIc	II d	2.622

Next nearest neighbor

O	O	Distance	O	O	Distance
Ia	IIa	4.063	Ic	IIc	3.592
Ia	II d	4.084	Ic	II d	4.243
Ib	IIc	4.197	IIa	IIc	3.675
Ib	II d	4.077	IIb	II d	3.857
Ic	IIb	3.272			

(c) O-Zr distances in the  $O_{Ic}$  coordination polyhedron

O	Zr	Distance
Ic	1	2.057
Ic	2	2.163
Ic	3	2.051

(d) Zr-Zr distances in the  $O_{Ic}$  coordination polyhedron

Zr	Zr	Distance
1	2	3.334
1	3	3.929
2	3	3.433

(e) O-Zr distances in the  $O_{II d}$  coordination polyhedron

O	Zr	Distance	O	Zr	Distance
II d	1	2.220	II d	3	2.285
II d	2	2.189	II d	4	2.151

Table 4 (cont.)

(f) Zr-Zr distances in the  $O_{IIa}$  coordination polyhedron

Zr	Zr	Distance	Zr	Zr	Distance
1	2	3.433	2	3	3.469
1	3	3.460	2	4	3.460
1	4	4.031	3	4	3.580

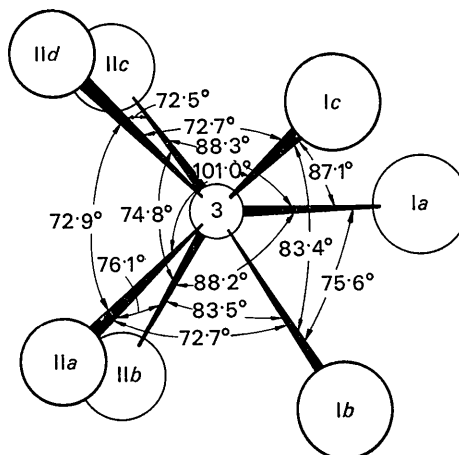
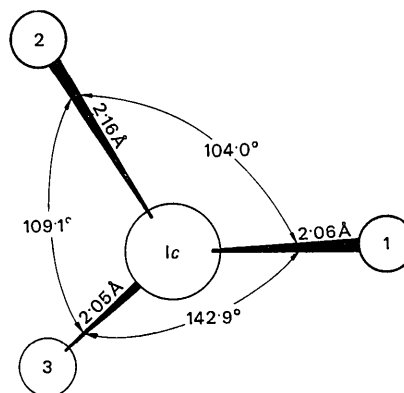
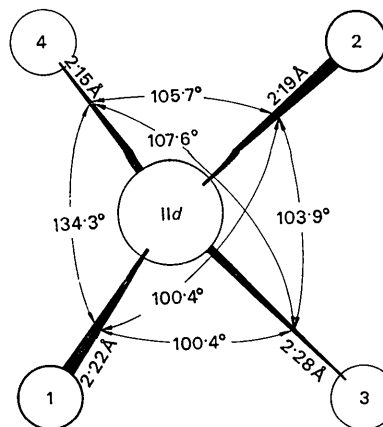
The most interesting feature of this structure is the sevenfold coordination of Zr. The Zr-O distances range from 2.05 Å to 2.28 Å. The next largest Zr-O distance is 3.58 Å, which cannot be considered in the coordination polyhedron. Fig. 3 shows the angles in this configuration. The  $O_{II}$  atoms in the group form a planar, square group which would correspond to one half of a normal eightfold cubic array. The  $O_I$  atoms form a triangle whose plane is nearly parallel to the plane of  $O_{II}$  atoms. The average Zr- $O_I$  distance is 2.07 Å, whereas the average Zr- $O_{II}$  is 2.21 Å. This difference is to be expected, as pointed out by McCullough & Trueblood, because Pauling's (1929) electrostatic valency rule predicts the relative bond strengths to be  $\frac{2}{3} : \frac{1}{2} = 4 : 3$ .

The details of the coordination configurations of the two oxygen atoms are shown in Figs. 4 and 5. The  $O_I$  atom is only 0.25 Å from the plane defined by the three Zr atoms to which it is coordinated. The triangular arrangement is not regular but has angles from 104° to 142°. This irregularity is due to two features of the structure. First, two  $O_I$  atoms share one edge of the configuration. This is the edge involving the 104° angle. Second, the steric hindrance of the other oxygen atoms in the layer prevents the movement of the third  $O_I$  atom into a more centrally located position.

The  $O_{II}$  coordination is nearly tetrahedral, with only one angle differing significantly from the tetrahedral angle of 109.5°. This deviation reflects the somewhat buckled nature of the plane of  $O_{II}$  atoms. This buckling is due to the influence of the lower coordination of the  $O_I$  atoms which results in a tipping of the  $ZrO_7$  groups as shown in Fig. 2.

The second interesting feature of this structure is the layer arrangement of atoms parallel to (100). The layers of  $O_{II}$  atoms are shown in Fig. 6 along with the layer of Zr atoms both above and below the  $O_{II}$  plane. This arrangement is only slightly distorted from the normal fluorite ( $CaF_2$ ) configuration. This portion of the  $ZrO_7$  polyhedra all shares edges with an average  $O_{II}$ - $O_{II}$  distance of 2.67 Å. Fig. 7 shows the  $O_I$  layer with the adjacent Zr atoms. This layer is quite irregular and only one  $O_I$ - $O_I$  edge is shared between adjacent  $ZrO_7$  polyhedra. The shared edge distance is 2.59 Å, in contrast to the other unshared  $O_I$ - $O_I$  distances of 2.83 Å and 2.80 Å in this layer. Fig. 8 shows the layer of  $ZrO_7$  polyhedra. In addition to the shared edges already mentioned, this figure shows the two  $O_I$ - $O_{II}$  edges which are also shared. Their values are both 2.58 Å in contrast to the average value for unshared  $O_I$ - $O_{II}$  edges which is 2.94 Å. These values show that the  $O_I$ - $O_I$  shared edge distance is the same as the

$O_I$ - $O_{II}$  shared edge distances. Both these values are less than the  $O_{II}$ - $O_{II}$  shared edge distances. The order for unshared edge distances, all of which are longer than the shared edges, is  $O_I$ - $O_I < O_I$ - $O_{II}$ . This sequence of distances is in agreement with the principles set forth by Pauling (1929) for ionic crystals as discussed by McCullough & Trueblood (1959).

Fig. 3. The angles and interatomic distances in the  $ZrO_7$  coordination polyhedron.Fig. 4. The angles and interatomic distances around the  $O_I$  atom.Fig. 5. The angles and interatomic distances around the  $O_{II}$  atom.

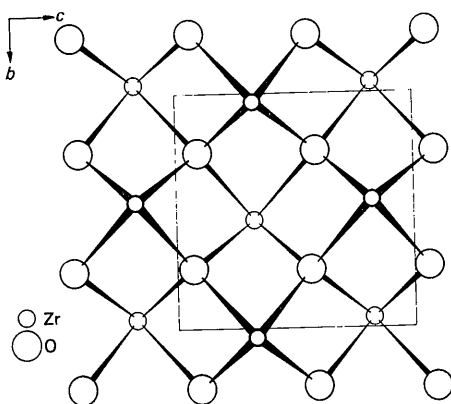


Fig. 6. The layer of O<sub>II</sub> atoms at  $x=0$  projected on the (100) plane. The Zr atoms above and below the plane are also included. The unit-cell outline represents its position at  $x=0$ .

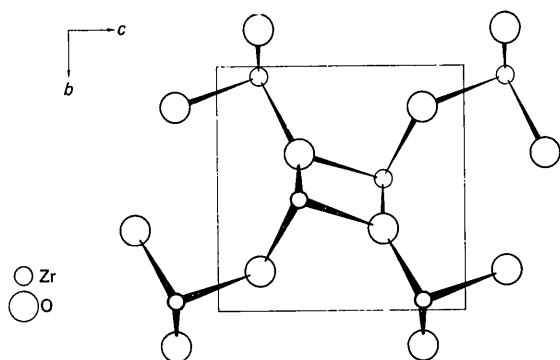


Fig. 7. The layer of O<sub>I</sub> atoms at  $x=1/2$  projected on the (100) plane. The Zr atoms above and below the plane are also included. The unit-cell outline represents its position at  $x=0$ .

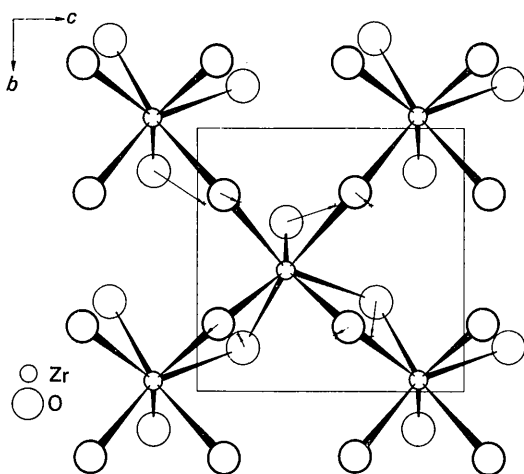


Fig. 8. The layer of ZrO<sub>7</sub> groups at  $x=1/4$  projected on the (100) plane. The unit-cell outline represents its position at  $x=0$ . The small crosses show the oxygen positions in the tetragonal form (see Fig. 10). The small arrows indicate the probable movement of oxygen at the phase change.

### Twinning

McCullough and Trueblood (1959) have interpreted the frequency of twinning in baddeleyite to be due to the relatively low energy difference between the ZrO<sub>7</sub> configuration found in the structure and another related arrangement, in which the group of three O<sub>I</sub> is rotated 180° about an axis approximately perpendicular to the plane defined by the four O<sub>II</sub> atoms. The implications of this interpretation require more detailed analysis to determine the relations across the twin plane. One important fact to be considered is the antiparallelism of the O<sub>I</sub> and O<sub>II</sub> planes with respect to the twin plane. A simple reflection of the structure across a plane parallel to (100) or a rotation about a twofold axis parallel to the  $c$  axis will not result in an acceptable twin boundary configuration. However, a very acceptable boundary may be obtained by rotating the structure about a twofold axis through  $x=1/2$ ,  $y=1/2$  and translating one half of the twin  $1/2a$  with respect to the other half. This arrangement is shown in Fig. 9. Notice that the composition plane is the plane of O<sub>II</sub> atoms. To understand the relationship of the McCullough & Trueblood interpretation to this boundary configuration, it is perhaps clearer to describe the alternative ZrO<sub>7</sub> group as a rotation of the O<sub>II</sub> group about an axis nearly perpendicular to the plane of the O<sub>I</sub> group. The distortion of the ZrO<sub>7</sub> groups at the composition plane results from an adjustment of the O<sub>II</sub> atoms to positions which are midway between the positions satisfying the stable configurations of each half of the twin. This shift is approximately 0.025 Å, and the resulting distortion is very small.

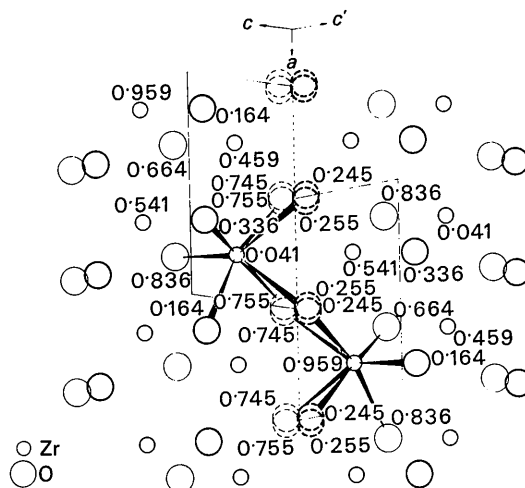


Fig. 9. Projection of (100) composition plane of the (100) twin of monoclinic ZrO<sub>2</sub>. The unit cell is partially outlined to indicate the  $1/2c$  glide condition at the boundary. The dotted circles representing oxygen atoms show positions for both halves of the twin. The final oxygen position will be an average of the two possibilities. The numbers represent the  $y$  coordinate for each atom in terms of  $b$ .

### Structural relations among the $ZrO_2$ polymorphs

Three polymorphs of  $ZrO_2$  have been well established. A second tetragonal phase has been reported by Garrett (1964), whose temperature stability region lies between the regions of the known tetragonal phase and the cubic phase. If this phase does exist, its structure is probably very similar to the structures of the established cubic and tetragonal phases, and the following discussion will not require any significant changes.

The tetragonal-cubic inversion temperature has been established by Smith & Cline (1962), using high temperature X-ray diffraction at  $2285 \pm 50$  °C with a maximum of 30° hysteresis. The narrow hysteresis suggests a displacive transformation, using the terminology of Buerger (1948). The displacive movements are easily visualized by comparing Figs. 10 and 11. The oxygen atoms of the tetragonal phase shift along the  $c$  axis to the planes  $z = \frac{1}{4}$  and  $\frac{3}{4}$  with a corresponding decrease in length of the  $c$  axis and an increase in length of the  $a$  axis until they become equal. No change in the bonding configurations is required.

The relationship of the monoclinic and tetragonal structures is not so straightforward. The most significant difference between the two structures is the change in coordination of the Zr atoms and one of the two O atoms which requires that some bonds be severed during the inversion. The large hysteresis observed for this transformation indicates the semi-reconstructive nature of the atomic readjustments, which may be seen by comparing Fig. 8 and Fig. 10. There is still some question about the relative orientations of the tetragonal and monoclinic structures, but the most likely correlation is the  $c$  axis of tetragonal form with the  $c$  axis of the monoclinic structures. In Fig. 8, the small crosses show the positions of the oxygen atoms in the tetragonal form superimposed on the central  $ZrO_7$  group of the monoclinic structure. The arrows show the most likely shifts which would take place during the transformation from monoclinic to tetragonal symmetry. The longest shift is the movement of the  $O_I$  atom attached to the  $ZrO_7$  group in the lower right of the figure to join the center group. This atom, which is initially 3.76 Å from the center Zr atom, moves about 1.2 Å. The whole transformation takes place by the rotation of the triangular groups of  $O_I$  atoms accompanied by minor movements of other atoms into the more symmetrical configuration. It is worthy of note that the oxygen atom which moves so as to join the new configuration is not the closest next nearest neighbor of the  $ZrO_7$  group. An  $O_I$  atom positioned directly below the square array of  $O_{II}$  atoms is only 3.58 Å from the Zr position.

Two studies describing the orientational relationships in single crystals of  $ZrO_2$  which have passed through the monoclinic-tetragonal inversion have been described by Bailey (1964) & Wolten (1964). The studies of Bailey involved thin films using electron microscopy and diffraction. Only the relationships

$c_m = c_t$  and  $b_m = a_t^*$  were observed. In contrast the work discussed by Wolten used isolated single crystals which were heated on a single-crystal orienter. The best crystal was twinned initially with one orientation dominating the volume. The tetragonal phase showed complex relationships with all three orthogonal directions showing both  $a_t$  and  $c_t$ . One set of vectors was found parallel to the old  $b_m$ , but neither of the other two sets were parallel to  $a_m$  or  $c_m$ . Instead they formed a 90° angle which was nearly symmetrically inscribed in the old monoclinic angle. On reversion, the monoclinic crystal was highly twinned. The two studies are somewhat contradictory. The relative sizes of the crystals used suggest that the strain fields in larger crystals used by Wolten may have masked the more expected results as observed by Bailey.

A recent phase equilibrium study of the monoclinic-tetragonal inversion in  $ZrO_2$  and  $HfO_2$  by Baun (1963) shows that monoclinic  $ZrO_2$  begins to change to tetragonal on heating around 1000 °C. The last trace of the monoclinic form disappears around 1180 °C. On cool-

\* The subscripts  $m$  and  $t$  refer to the monoclinic and tetragonal phases respectively. The vector  $a_t$  refers to  $a_1 + a_2$  according to the Teufer (1962) unit cell.

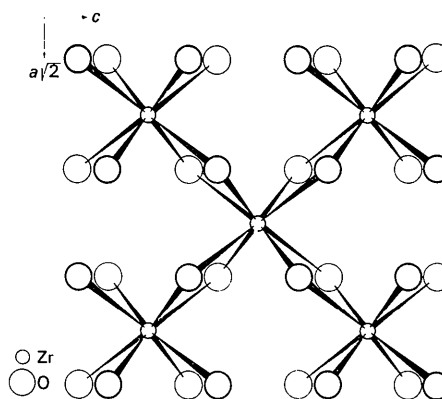


Fig. 10. One layer of  $ZrO_8$  groups in the tetragonal  $ZrO_2$  structure. The plane of projection is (110).

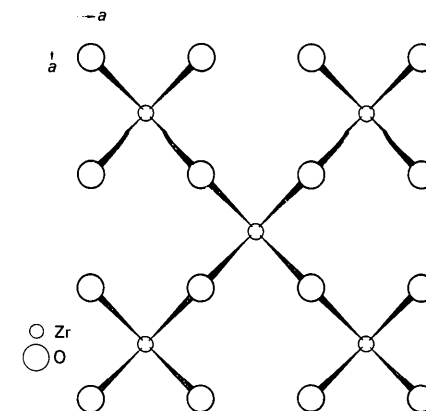


Fig. 11. One layer of  $ZrO_8$  groups in the cubic  $ZrO_2$  structure. The plane of projection is (100).



ing, the monoclinic form first appears at 970 °C, and the tetragonal phase disappears at 750 °C. For HfO<sub>2</sub> these ranges are 1500–1600 °C and 1550–1450 °C respectively. A most remarkable feature is the overlap of the ranges for HfO<sub>2</sub>. The tetragonal HfO<sub>2</sub> first appears on heating at a temperature below that which the monoclinic form first appears on cooling. There is some question as to whether the tetragonal forms of ZrO<sub>2</sub> and HfO<sub>2</sub> are isostructural, but because of their other similarities, there is little reason at present to doubt the structural similarity. The lack of 'extra' diffraction maxima in the tetragonal high temperature X-ray patterns, as reported by Baun, could well be due to the higher atomic scattering factor of Hf compared with Zr. Because the ratio of scattering of Hf to O will be greater than for Zr to O and because the weak lines are all due to oxygen contributions, assuming the tetragonal arrangement by Teufer (1962) for ZrO<sub>2</sub> is true for HfO<sub>2</sub> also, they would be relatively weaker in the HfO<sub>2</sub> phase than in the ZrO<sub>2</sub> phase.

If this overlap of stability fields for HfO<sub>2</sub> is true, the phase inversion cannot be a simple, single-stage transformation. One possibility, which would explain this apparent overlap, is the development of an intermediate mixed layer structure in the transition region. It may be that all the O<sub>I</sub> layers do not readjust to the fluorite configuration at the same temperature. Alternatively, every second, third, or fourth layer may transform first, and, subsequently, the intervening layers complete their transformation at a higher temperature. Such a transformation might develop polytypes analogous to those observed in the wurtzite and sphalerite type compounds. If the stacking of layers were regular, superstructure lines should appear in the X-ray pattern. However, if the stacking is random, superstructure lines from any ordering would be weak and difficult to observe.

This discussion would appear to apply equally well to the monoclinic–tetragonal transformation in ZrO<sub>2</sub>. The hysteresis is larger for ZrO<sub>2</sub> than for HfO<sub>2</sub>, but only 30 °C lies between temperature of first appearance of tetragonal ZrO<sub>2</sub> on heating and the monoclinic form on cooling. This is a very narrow temperature range for a transformation which otherwise appears so sluggish. It may, however, be an indication that if equilibrium conditions were obtained by the transformation,

then an overlap of monoclinic and tetragonal phases would be observed, and thus the phase relations would be the same as observed for HfO<sub>2</sub>.

The authors would like to acknowledge the very capable assistance of Mr Philip M. Salter, who collected the intensity data and helped in some of the data processing. Also several discussions with Prof. J. D. McCullough proved most valuable in understanding some problems encountered in the structural analysis as well as the structural relations of the various polymorphs.

This work was performed under the auspices of the U.S. Atomic Energy Commission.

#### References

- ADAM, J. & ROGERS, M. D. (1959). *Acta Cryst.* **12**, 951.  
 BAILEY, J. E. (1964). *Proc. Roy. Soc. A*, **279**, 395.  
 BAUN, W. L. (1963). *Science*, **140**, 1330.  
 BUERGER, M. J. (1948). *Amer. Min.* **33**, 101.  
 COHEN, I. & SCHANER, B. E. (1963). *J. Nucl. Mat.* **9**, 18.  
 DAUBEN, C. H. & TEMPLETON, D. H. (1955). *Acta Cryst.* **8**, 841.  
 GANTZEL, P. K., SPARKS, R. A. & TRUEBLOOD, K. N. (1961). Program Number 317, Amer. Cryst. Assn. Program Listing, 2nd Ed., Nov. 1961.  
 GARRETT, H. J. (1964). *X-ray Study of Tetragonal Monoclinic Inversion in ZrO<sub>2</sub>*. Paper 40-B-63, 65th Annual Meeting, Amer. Ceram. Soc., Pittsburgh, Pa., April 27–May 2, 1963.  
 HOERNI, J. A. & IBERS, J. A. (1954). *Acta Cryst.* **7**, 744.  
 JAMES, R. W. & BRINDLEY, G. W. (1931). *Phil. Mag.* **12**, 81.  
 MCCULLOUGH, J. D. & TRUEBLOOD, K. N. (1959). *Acta Cryst.* **12**, 507.  
 NARAY-SZABO, I. (1936). *Z. Kristallogr.* **94**, 414.  
 PAULING, L. (1929). *J. Amer. Chem. Soc.* **51**, 1010.  
 SMITH, D. K. & CLINE, C. F. (1962). *J. Amer. Ceram. Soc.* **45**, 249.  
 TEUFER, G. (1962). *Acta Cryst.* **15**, 1187.  
 THOMAS, L. H. & UMEDA, K. (1957). *J. Chem. Phys.* **26**, 293. (See also *International Tables for X-ray Crystallography*, Vol. III, 210-2. Birmingham: Kynoch Press (1962)).  
 TULINSKY, A., WORTHINGTON, C. R. & PIGNATARO, E. (1959). *Acta Cryst.* **12**, 623.  
 WEBER, B. C. (1962). *Acta Cryst.* **15**, 1187.  
 WOLTEN, G. M. (1964). *Acta Cryst.* **17**, 763.  
 YARDLEY, K. (1926). *Miner. Mag.* **21**, 169.